2011 International Conference on Nanotechnology and Biosensors
IPCBEE vol.25(2011) © (2011) IACSIT Press, Singapore

An Intensity-Interrogated Sensing Technique Based on Porous Silicon Microcavity

Chao Wu, Guoguang Rong [+], Junteng Xu and Guoxing Wang

School of Microelectronics, Shanghai Jiao Tong University, Shanghai 200240, China

Abstract. Porous silicon is a versatile platform for developing label-free biosensors with high sensitivity and low cost. In this work, fabrication conditions are carefully tuned to produce a resonant structure, or microcavity with the best quality that can be obtained. More importantly, we investigated the possibility of using the intensity-interrogated sensing technique in liquid form, which is rarely reported before. Using glucose as a target, this method is demonstrated to be effective in lowering practical detection limit while achieving high reliability simultaneously. The limit is reduced from approximately 7×10^{-4} RIU to 7×10^{-5} RIU compared to the red shift method. In this way we demonstrate this technique is preferred to the much used red shift method in practical sensing tasks.

Keywords: porous silicon; intensity-interrogated; microcavity

1. Introduction

First proposed by Sailor et al. [1], potential application of porous silicon (PSi) in the biomedical field is extensively exploited ever since [2]-[11]. Apart from its large surface area, it is especially interested in the label-free optical biosensing area, attributing to tunable optical properties and variable surface chemistry. This sponge-like material to date has been tailored to detect chemicals [2, 3], biomolecules (DNA [4, 5], proteins [6]) and even organisms [7] in various motifs: waveguides [8], ellipsometry [9], Fabry-Pérot fringes based on different structures, from single layer [1], multilayer [10], rugate filter [11], to microcavity (MC) [4]. Among these, microcavity is especially interesting due to its strong confined field, making it a promising architecture to achieve high sensitivity.

Porous silicon based microcavity is implemented by embedding a central layer between two distributed Bragg reflectors (DBRs). The DBRs are stacks of several periods of λ/4-thick low and high porosity layers. Here the effective optical thickness (EOT = n×d) of central layer is λ/2 thick. This resonant structure can localize light with a wavelength of λ in its cavity layer, thus is more sensitive to cavity optical thickness change (e.g. caused by biomolecules infiltration and binding) when compared with evanescent field techniques such as surface plasma resonance (SPR). Besides, the sharp resonance peak makes it easier to resolve small EOT changes comparing to DBR or rugate filters. Beyond the inherent strong field-molecule interactions, the nanocrystalline matrix offer more binding sites in its 3-D architecture, resulting in large dynamic range.

In this study, we mainly investigate the feasibility of intensity-interrogated sensing technique. In order to avoid the "interference factors" in a specific sensing task, in which sensitivity may be compromised by different target-probe affinity and intricate sensing procedures, we simply use aqueous glucose solutions diluted into different concentrations as targets. Using a set of self-made equipment, we plot charts of reflectance variation versus time, or sensorgrams. By comparing them with those red shift data, we are able

[+] Corresponding author. Tel.: + 86-21-34204748-1028; fax: + 86-21-34204719.
E-mail address: guoguangrong@ic.sjtu.edu.cn.

to testify the superiority of intensity-interrogated approach over commonly used red shift method both in terms of detection resolution and reliability.

2. Experimental

2.1. Microcavity Preparation

It has become a common practice to fabricate PSi by anodizing crystalline silicon in hydrofluoric acid solution. In this experiment, devices are fabricated from heavily boron-doped (p+) <100>-oriented silicon wafers with a resistivity of 0.01 Ω·cm in ambient conditions. The electrochemical process proceeds in a mixture of 95% ethanol (64%) and 41.2% aqueous HF acid (36%), which yields a 15% HF electrolyte. A LabVIEW^{TM}-controlled Keithley's Model 2400 SourceMeter® is used to apply an alternating constant current. As is listed in Table 1, appropriate etching time and current density are chosen to realize the photonic bandgap structure. In this study, a microcavity sample with 5-period DBRs is prepared for subsequent examine of the intensity-interrogated method. Its thickness is estimated to be ~2.5μm.

Table 1. Microcavity Parameters

Device Architecture		Porosity	Layer Thickness (nm)	Current Density (mA/cm^2)	Etch Time (s)
DBR Stack	HP Layer	89%	123	80	2.3
	LP Layer	60%	78	20	6.9
Central Layer		89%	246	80	4.6

HP: high porosity; LP: low porosity

2.2. Post-etch Treatment

As is mentioned before, PSi microcavity has to undergo a series of post-etch treatments before finally executing a detection task. It generally includes a KOH soaking to enlarge pore size to facilitate biomolecules' infiltration, oxidation to introduce a hydrophilic surface, and necessary surface chemistry modifications (e.g. receptor immobilization) [12]. Considering we are investigating PSi pores infiltrated with aqueous glucose solution and the target molecule is small enough (~1nm) [13] comparing with the pore diameter (20~30nm) [12], we skip the KOH soaking and receptor immobilization procedures and only carry out oxidation.

Freshly etched PSi surface is massively Si-H_x terminated, which is a metastable bond gradually uptook by oxygen at room temperature (aging) [14], resulting in undesirable drift of resonance peak. Moreover, hydride-covered surface is hydrophobic and inhibit analyte from diffusion into the spongy material. Thus, the oxidation step is in a sense compulsory. Nevertheless, it is hard to evaluate its impact on device performance when calculating each layer's theoretical thickness, thus the resonant structure is off tune and certain degree of degradation may ensue. However, it is beneficial to reduce oxide thickness in the PSi matrix so long as universal oxide coverage is guaranteed in the first place. To this end, we propose to oxidize PSi samples at a reduced temperature, which, in this experiment, is 500°C for 30min.

2.3. Sensing System Implementation

As is illustrated in Fig.1, intensity-interrogated sensing is basically realized with a flow cell, a peristaltic pump, and a spectrophotometer to record signals. The flow cell comprise of a cover glass of 0.25mm thick and a PSi microcavity with a round sensing area of ~2cm^2, spaced by an o-ring of approximately 1mm in height, and syringe needles as the inlet and outlet. This configuration provides a convenient way to investigate the response of microcavity even though relatively large sample volume is consumed (totaling about 0.2mL in the chamber). This problem can be easily circumvented by integrating smaller transducer with corresponding fluid handling system.

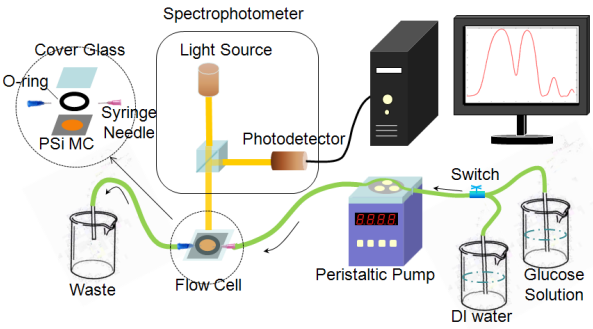

Fig. 1: Schematic view of the intensity-interrogated sensing system. Disassembled flow cell is also shown in the upper-left inset.

3. Results and Discussions

3.1. Spectra of Microcavity

Fig.2 shows reflectance spectra of a PSi microcavity with two 5-period DBRs. The maximum reflectance sees only minor reduction after oxidation, but full-width at half maximum (FWHM) decreases from ~17 to ~13, due to smaller refractive index (RI) of SiO_2 with regard to Si, which decreases the RI ratio between HP and LP layers (n_{HP}/n_{LP}) [15]. The resonance wavelength blue shifts from 643nm (black) to 580nm (red), which drifts, on average, 60~70nm from sample to sample, smaller than that reported in reference [12]. This is attributed to fewer crystalline silicon left to oxidize in high porosity bilayers (89%/60%), and probably, thinner oxides on pore walls. No peeling or destruction is observed with such high porosities. Microcavities, especially its central layers, fabricated with large air volume allow more analyte to interact with confined light field, thereby engendering intensified outputs. Total oxide coverage at reduced oxidation temperature is substantiated by the small blue shift (~2nm) upon half a year's storage (blue). In this way the sensor suffers smaller degradation in terms of resonance quality after post-etch treatments. Besides, sensor performance can be further optimized by substituting the pore RI with 1.3330 (RI of water at λ=589nm in a temperature of 20°C [16]) in calculating EOT of each layer, because biosensing is often operated in aqueous environment.

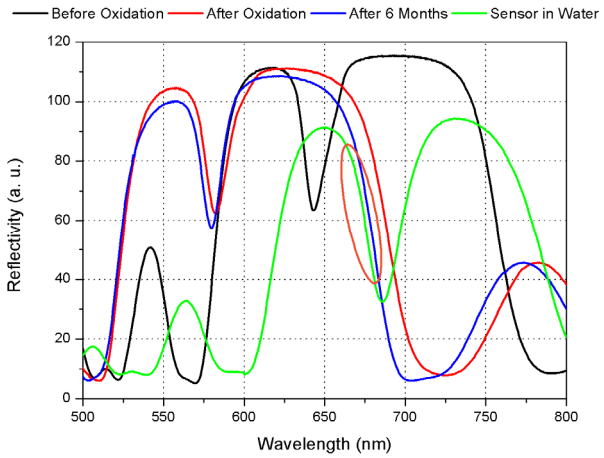

Fig. 2: Reflectance spectra of a PSi microcavity before (black) and after oxidation (red). The resonance peak undergoes only ~2nm blue shift after 6 months' storage (blue), exhibiting excellent stability. Reflectivity of the sample soaked in water is reexamined 6 months later, which is shown in green. The linear part used in the intensity-interrogated experiment is indicated with a brown circle. This sample is constructed with 5-period DBRs and designed to work at a resonance wavelength of 650nm.

3.2. Sensorgrams

Fig.2 also shows the spectrum after the PSi microcavity is assembled into the flow cell and then soaked in water. A FWHM broadening from ~13nm (blue) to ~24nm (green) is observed compared with the dry sample. In this experiment, the left linear segment of the resonance peak (circled in brown) is found the

largest in slope (3.1R%/nm), indicating largest achievable sensitivity. Expanding bidirectionally from the midpoint, we linear fitted the circled curve, and determine the linear range to be ~11nm (from 672nm to 683nm), demarcated by a 0.6% fitting residual (3.1R%/nm × 0.2nm, 0.2nm is the resolution of the spectrophotometer). The detection wavelength is then fixed at a point (683nm in this experiment) near the upper boundary of the linear range to guarantee largest dynamic range, because the RI of glucose solution is larger than that of water, which will red shift the fringes.

With detection wavelength fixed, a sensorgram of reflectivity vs. time is recorded using the intensity-interrogated technique. Fig.3(a) shows three sensing curves of this kind in response to 5wt%, 10wt% and 20wt% glucose solutions. A tolerance band of 0.1% is set to determine whether the sensor reaches its final stable states. The 20wt% curve is also used as an example to illustrate response time (τ_{res}) and regeneration time (τ_{reg}). They are defined as the time elapsed when the output signal changes 70% from its previous state to the final state [17]. The regeneration time is far longer than response time, which is attributed to the slow out-diffusion process during the regeneration period, during which analyte is bogged down within the nanocrystalline matrix.

3.3. Optical Outputs

After recording sensorgrams of four glucose concentrations (i.e. 0.1wt%, 0.5wt%, 1wt% and 5wt%), we read the reflectivity changes (ΔR%) and plot them in black dots in Fig.4. With the same set up, we also record spectra like those in Fig.2 and map resonance peak red shifts (Δλ) in Fig.4 in blue. All the data are repeated three times and linear fitted.

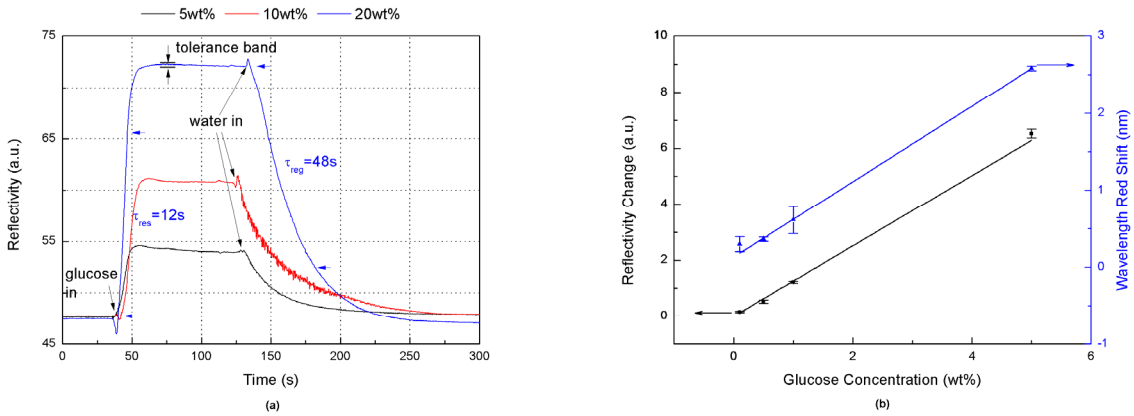

Fig. 3: (a) Intensity-interrogated detection of glucose with a concentration of 5wt%, 10wt% and 20wt% respectively. Response time (τ_{res}), regeneration time (τ_{reg}) and tolerance band are also shown with respect to the 20wt%curve. (b) Optical response of PSi microcavity versus four glucose concentrations, 0.1wt%, 0.5wt%, 1wt% and 5wt%. Black dots are extracted from sensorgrams as those shown in (a). The resonance peak red shift is drawn in blue. All data are linear fitted with the error bar shown in the chart.

With the assistance of Fig.3(b), now we are able make a straightforward comparison of the intensity-interrogated and the red shift method. Generally speaking, the error bars drawn with those ΔR% data are much shorter than the Δλ's, implying higher reliability of the intensity-interrogated approach. Besides, we are able to obtain information from the sensorgrams on when equilibrium is established and record highly reliable data by averaging data within the tolerance band or employing other advanced data processing algorithms. More importantly, red shift for 0.1wt% completely overlaps with that of 0.5wt% in Fig.3(b), virtually making those two concentrations indistinguishable. Thus the practical detection limit of this method is ~0.5wt%, or about 7×10^{-4} RIU change [16]. By comparison, the two solutions can be easily resolved with the intensity-interrogated technique, thereby allowing the detection limit to be pushed down to 0.05wt%, or about 7×10^{-5} RIU. In this way we can see the much used red shift technique may become problematic in practical sensing applications, where useful signal may be overwhelmed by various noises.

4. Conclusions

In this work, after obtaining high quality PSi microcavity, we employ the intensity-interrogated sensing technique rather than the much used red shift method in determining glucose concentration. This proves to be advantageous in terms of high reliability and, more importantly, lowering detection limit with the same facility. In this manner, an order of magnitude reduction in the actual detection limit is attained ($\sim 7\times10^{-4}$ RIU down to $\sim 7\times10^{-5}$ RIU). This result suggests more frequent use of intensity-interrogated technique in practical sensing tasks. It may even serve as a major solution for the commercialization of porous silicon biosensors.

5. Acknowledgements

The authors would like to acknowledge funding support from Shanghai Municipal Natural Science Foundation No. 11ZR1418300.

6. References

[1] V. S.-Y. Lin, K. Motesharei, K. Motesharei, K.-P. S. Dancil, M. J. Sailor, and M. R. Ghadir. A porous silicon-based optical interferometric biosensor. *Science* 1997, **278**: 840-843.

[2] V. Mulloni, L. Pavesi. Porous silicon microcavities as optical chemical sensors. *Appl. Phys. Lett.* 2000, **76**: 2523.

[3] F. Cunin et al. Biomolecular screening with encoded porous-silicon photonic crystals. *Nature Mater.* 2002, **1**: 39-41.

[4] S. Chan, P. M. Fauchet, Y. Li, L. J. Rothberg, B. L. Miller. Porous silicon microcavities for biosensing applications. *Phys. Stat. Sol. A*. 2000, **182**: 541-546.

[5] G. Rong, J. D. Ryckman, R. Mernaugh and S.M. Weiss. Label-free porous silicon membrane waveguide for DNA sensing. *Appl. Phys. Lett.* 2008, **93**: 161109.

[6] K-P. S. Dancil, D. P. Greiner, M. J. Sailor. A porous silicon optical biosensor: Detection of reversible binding of IgG to a protein A-modified surface. *J. Am. Chem. Soc.* 1999, **121**: 7925-7930.

[7] S. D. Alvarez et al. Using a porous silicon photonic crystal for bacterial cell-based biosensing. *Phys. Stat. Sol. A.* 2007, **204**: 1439-1443.

[8] G. Rong, J. J. Saarinen, J. E. Sipe, and S. M. Weiss. High sensitivity sensor based on porous silicon waveguide. *Mater. Res. Symp. Proc.* 2006, **934**: 64 - 69.

[9] S. Zangooie, R. Bjorklund, H. Arwin. Vapor sensitivity of thin porous silicon layers. *Sens. Actuators B.* 1997, **43**: 168-174.

[10] C. Pacholski, M. Sartor, M. J. Sailor, F. Cunin, G. M. Miskelly. Biosensing using porous silicon double-layer interferometers: reflective interferometric Fourier transform spectroscopy. *J. Am. Chem. Soc.* 2005, **127**: 11636-11645.

[11] E. Lorenzo et al. Porous silicon-based rugate filters. *App. Opt.* 2005, **44**: 5415-5421.

[12] L. A. DeLouise and B. L. Miller. Trends in Porous Silicon Biomedical Devices - Tuning Microstructure and Performance Trade-offs in Optical Biosensors. *Proc. SPIE.* 2004, **5357**: 111-125.

[13] A Sense of Scale, (2007). Available at: http://www.falstad.com/scale/ (Accessed: 31 Aug 2011).

[14] D. Graf, M. Grundner, R. Schulz, and L. Mulhoff. Oxidation of HF-treated Si wafer surfaces in air. *J. Appl. Phys.* 1990, **68**: 5155-5161.

[15] L. Pavesi. Porous silicon dielectric multilayers and microcavities. *La Rivista del Nuovo Cimento.* 1997, **20**: 1-76.

[16] W. M. Haynes. *CRC Handbook of Chemistry and Physics, 91st Edition*. CRC Press, 2010.

[17] J. J. Carr. *Sensors and circuits*. Prentice Hall, 1993.